Acta Pharmaceutica Sinica B 2022;12(1):316–325

Chinese Pharmaceutical Association
Institute of Materia Medica, Chinese Academy of Medical Sciences

Acta Pharmaceutica Sinica B

www.elsevier.com/locate/apsb
www.sciencedirect.com

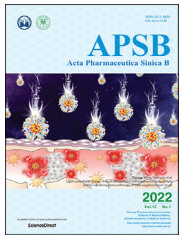

ORIGINAL ARTICLE

A NIR fluorescent probe for Vanin-1 and its applications in imaging, kidney injury diagnosis, and the development of inhibitor

Zhenhao Tian[a,b,c,†], Fei Yan[a,†], Xiangge Tian[a,b,†], Lei Feng[a,d,*], Jingnan Cui[e], Sa Deng[a], Baojing Zhang[a], Tian Xie[f,*], Shanshan Huang[a], Xiaochi Ma[a,b,*]

[a]*Dalian Key Laboratory of Metabolic Target Characterization and Traditional Chinese Medicine Intervention, The Second Affiliated Hospital, College of Integrative Medicine, College of Pharmacy, Dalian Medical University, Dalian 116044, China*
[b]*Jiangsu Key Laboratory of New Drug Research and Clinical Pharmacy, Xuzhou Medical University, Xuzhou 221004, China*
[c]*School of Life Sciences, Northwestern Polytechnical University, Xi'an 710072, China*
[d]*School of Chemistry and Chemical Engineering, Henan Normal University, Xinxiang 453007, China*
[e]*State Key Laboratory of Fine Chemicals, Dalian University of Technology, Dalian 116024, China*
[f]*College of Pharmacy, Key Laboratory of Elemene Class Anti-Cancer Chinese Medicines, Hangzhou Normal University, Hangzhou 311121, China*

Received 18 February 2021; received in revised form 22 April 2021; accepted 27 May 2021

KEY WORDS

Vanin-1;
NIR fluorescent probe;
Kidney injury diagnosis;
Fluorescence imaging;
Oleuropein

Abstract Vanin-1 is an amidohydrolase that catalyses the conversion of pantetheine into the aminothiol cysteamine and pantothenic acid (coenzyme A precursor), which plays a vital role in multiple physiological and pathological processes. In this study, an enzyme-activated near-infrared (NIR) fluorescent probe (DDAV) has been constructed for sensitively detecting Vanin-1 activity in complicated biosamples on the basis of its catalytic characteristics. DDAV exhibited a high selectivity and sensitivity toward Vanin-1 and was successfully applied to the early diagnosis of kidney injury in cisplatin-induced kidney injury model. In addition, DDAV could serve as a visual tool for *in situ* imaging endogenous Vanin-1 *in vivo*. More importantly, *Enterococcus faecalis* 20247 which possessed high expression of Vanin-1 was screened out from intestinal bacteria using DDAV, provided useful guidance for the rational use of NSAIDs in clinic. Finally, oleuropein as a potent natural inhibitor for Vanin-1 was discovered from

*Corresponding authors. Tel./Fax: +86 411 86110419.
E-mail addresses: leifeng@dmu.edu.cn (Lei Feng), xbs@hznu.edu.cn (Tian Xie), maxc1978@163.com (Xiaochi Ma).
†These authors made equal contributions to this work.
Peer review under responsibility of Chinese Pharmaceutical Association and Institute of Materia Medica, Chinese Academy of Medical Sciences.

https://doi.org/10.1016/j.apsb.2021.06.004

herbal medicines library using a high-throughput screening method using DDAV, which held great promise for clinical therapy of inflammatory bowel disease.

1. Introduction

Vanin-1 (EC 3.5.1), also known as pantetheinase, is an epithelial glycosylphosphatidylinositol (GPI)-anchored ectoenzyme which catalyzes the cleavage of pantetheine into the amino-thiol cysteamine and pantothenic acid (vitamin B5, the coenzyme A precursor)[1,2]. Importantly, Vanin-1 plays a vital role in multiple physiological and biological processes ranging from gluconeogenesis, pantothenic acid recycling, and cell migration, as well as oxidative stress regulation and inflammation aggregation in various pathological status[3−7]. It has a wide expression in different organs, especially in kidney and intestine[8−10]. Recent studies reveal that Vanin-1 expression is tightly intertwined with occurrence and development of certain diseases, such as kidney injury, hepatotoxicity, inflammatory bowel disease (IBD), diabetes and malaria[8,10]. In view of the powerful functions of Vanin-1 and growing body of evidence, urinary Vanin-1 is regarded as a predictive biomarker for various kidney diseases, including drug-induced renal injury, acute kidney injury and diabetic nephropathy[11−13]. In addition, as a major regulator of intestinal inflammation, Vanin-1 is also recognized to be a potential therapeutic target as a new anti-inflammatory strategy[14]. Collectively, it is imperative to develop efficient tools for rapid and accurate tracing endogenous Vanin-1 activity in complex biosystems, which should be invaluable in further exploring Vanin-1's pathophysiology function and related diseases.

Traditional analysis methods for Vanin-1 including radioactive isotope labeling and spectrophotometric assay are chiefly based on the quantification of cysteamine[15,16], which are not applicable for *in situ* dynamic determining enzyme's bioactivity, due to insufficient sensitivity and laborious measurement procedure. Recently, fluorescence/bioluminescence-based analytical technology has received considerable attention for the advantages of simplicity, superb selectivity/sensitivity, real-time visualization, and non-invasive detecting[17−25]. For Vanin-1, few probes have been designed and developed for detecting Vanin-1 in cells and mice recently. For example, Lin et al.[26] constructed a bioluminogenic sensor based on aminoluciferin, Qian et al.[27,28] developed two NIR emission ratio fluorescent probes for sensing Vanin-1. Lately, Yang et al.[29] constructed a NIR probe for bioimaging Vanin-1 and demonstrated the increase of Vanin-1 level in the tissues of mouse inflammatory models. However, there is rare fluorescent probes have been developed for exploring the vital function of Vanin-1 in the aspect of kidney injury diagnosis, inflammatory prevention and therapy, intestinal bacteria and inhibitor screening.

As is known, fluorescent probe with near-infrared (NIR) emission is widely regarded as an ideal candidate for bioimaging in living system due to its superiorities of deep tissue penetration and minimum background autofluorescence[30−35]. Herein, based on the catalytic characteristics of Vanin-1, a novel NIR fluorescent probe DDAV was designed and developed by conjugating pantothenic acid with the NIR fluorophore DDAN. DDAV exhibited low cytotoxicity and ultra-sensitivity/specificity, which acted as a practical tool for real-time detecting Vanin-1 activity *in vitro* and *in vivo*. Furthermore, DDAV was employed to monitor kidney function and diagnosis of kidney injury by detecting the Vanin-1 levels in urine. In addition, DDAV could realize the *in vivo* imaging of Vanin-1 in living animals, and further screening out functional intestinal bacteria which had a high expression of Vanin-1. At last, using DDAV, a high-throughput screening method for Vanin-1 inhibitors was established, and oleuropein as a novel natural inhibitor from herbal medicines library that possessed remarkable inhibitory effect toward Vanin-1 was discovered, which would hold a promising application for clinical treatment of inflammatory bowel disease.

2. Materials and methods

2.1. Materials

All chemicals were obtained from qualified reagent supplies with analytical reagent grade and used without further purification. Vanin-1 was purchased from Novoprotein Scientific Inc. (Shanghai, China). Cisplatin, carbonic anhydrase (Cas), dipeptidyl peptidase 4 (DPP4), leucine aminopeptidase (LAP), human serum albumin (HSA), β-glucosidase (β-Glc), β-galactosidase (β-Gla), β-glucuronidase (GLU), proteinase K (PK), carboxylesterases (CE1b, CE1c, CE2), bovine serum albumin (BSA) and lysozyme (Ls) were purchased from Sigma−Aldrich (St. Louis, MO, USA). Cytochrome P450 3A4 (CYP3A4) was supplied by Cypex (Dundee, UK). Pooled human brain S9 (HBS9), pooled human lung S9 (HLuS9), pooled human intestine S9 (HIS9), pooled human kidney S9 (HKS9), and pooled human liver S9 (HLS9) were purchased from the Rild Research Institute for Liver Diseases (Shanghai, China). Glucose, lysine (Lys), serine (Ser), glutamine (Gln), glycine (Gly), arginine (Arg), tryptophan (Trp), myristic acid, tyrosine (Tyr), cysteine (Cys), glutathione (GSH), glutamate (Glu), bis (*p*-nitrophenyl) phosphate (BNPP) and loperamide (LPA) were purchased from Shanghai Yuanye Bio-Technology (Shanghai, China). β-Lapachone was obtained from Bide Pharmatech Ltd. (Shanghai, China). Ketoconazole was purchased from J&K Chemicals (Beijing, China). Creatinine kits and blood urea nitrogen kits were obtained from Nanjing jiancheng biological engineering research institute (Nanjing, China). LoVo cells (human colon carcinoma cell line) and MCT cells (mouse renal proximal tubule cell line) were purchased from ATCC (Manassas, USA). Anti-fluorescence quenching sealant was obtained from Beyotime Biotechnology (Shanghai, China). 4′,6-Diamidino-2-phenylindole (DAPI) was obtained from Vector Laboratories (USA).

2.2. Synthesis of fluorescent probe DDAV

The fluorescent probe DDAV was synthesized according to the synthetic route as shown in Supporting Information Scheme S1.

2.3. The application of DDAV in cisplatin-induced acute kidney injury model

All protocols for this animal study conformed to the Guide for the Care and Use of Laboratory Animals. All animal experiments were carried out in accordance with guidelines approved by the ethics committee of Dalian Medical University (Dalian, China). C57BL/6 mice (6−8 weeks, 18−22 g), provided by the Experimental Animal Center of Dalian Medical University (Dalian, China), were housed under diurnal lighting condition with 12 h of light and subjected to a standard normal diet with receiving water ad libitum. Mice were divided into two groups (control group and cisplatin group, $n = 5$) randomly. Cisplatin group mice were intraperitoneally administration with cisplatin (1.0 mg/mL, prepared in normal saline) with 15 mg/kg dosage administration. Meantime, control group mice received an intraperitoneal injection of equal amount of normal saline. The urine of experimental mice was collected by metabolic cages for every 24 h. After cisplatin injecting for 72 h, kidneys and blood of the experimental mice were harvested.

Both serum creatinine (sCr) and blood urea nitrogen (BUN) were investigated based on corresponding commercial kits. The Vanin-1 activity in urine was measured in the mixed system with a final incubation volume of 0.2 mL consisting of potassium phosphate buffer (100 mmol/L, pH 7.4), 2 μL of stock solution of DDAV (10 μmol/L) and 20 μL mouse urine. After incubation at 37 °C for 1 h in a thermostat, the reaction was quenched by addition of ice acetonitrile (100 μL), and the mixtures were then centrifuged at 20,000×g at 4 °C for 20 min. After that, the aliquots of supernatant were collected and used for fluorescence analysis. Control experiments without mouse urine were carried out which using equal volume potassium phosphate buffer replacing urine sample. The protein level of experimental mice urine was evaluated by SDS-PAGE (SDS-polyacrylamide gel electrophoresis), and the gel was stained with Coomassie brilliant blue.

In addition, the renal histopathologic features were investigated. Before embedded in paraffin for 72 h, the kidney specimens from the two groups of experimental mice were fixed in 10% buffered formalin for 24 h. After that, the kidney sections of 10 μm thickness were subjected to Hematoxylin and Eosin (H&E) staining in accordance with the manufacturer's instructions, which were then photographed by an Axioplan 2 Imaging system. The histological examinations were conducted blind.

2.4. Imaging of Vanin-1 in mice

BALB/C mice (6−8 weeks, 18−22 g) were provided by the Experimental Animal Center of Dalian Medical University (Dalian, China). Mice were randomly divided into two groups ($n = 3$), normal group: mouse was subjected to an intraperitoneal injection of DDAV (200 μL, 40 μmol/L in normal saline), inhibition group: mouse was subjected to co-administration of DDAV (40 μmol/L) and β-lapachone (200 μmol/L) in normal saline 200 μL intraperitoneally. Next, these mice were anesthetized and then scanned using Night OWL II LB983 *in vivo* imaging system at the different time interval within 20 min, with an excitation laser of 605 nm and an emission filter of 660 nm. In addition, the abdominal cavity of probe-treated group mice was exposed for further imaging under the same imaging conditions.

2.5. The distribution of Vanin-1 in intestine

Randomly number BALB/c mice 1−5 and collected fresh feces. The mice were oral administration mixed antibiotic: neomycin sulfate, vancomycin and metronidazole with 10 mg/kg dosage administration every 12 h; added cephalexin 100 mg/mL in water. After mixed antibiotic administration for a week, fresh feces were collected. One part of feces was coated on Luria−Bertani (LB) agar plate, the other part was collected for lyophilization. Crushed the lyophilized feces and added PBS buffer to 20 mg/mL, the mixtures were then centrifuged at 1000×g at 4 °C for 10 min after vortex, and the supernatant was collected as feces S9. The Vanin-1 activity in feces was measured in the mixed system with a final incubation volume of 0.2 mL consisting of potassium phosphate buffer (100 mmol/L, pH 7.4), 2 μL of stock solution of DDAV (10 μmol/L) and 50 μL feces S9. After incubation at 37 °C for 1 h in a thermostat, the reaction was quenched by addition of ice acetonitrile and the mixtures were centrifuged at 20,000×g at 4 °C for 20 min. After that, the aliquots of supernatant were collected and used for fluorescence analysis. All assays were carried out in duplicates.

2.6. The screening of intestinal bacteria

Initially, prepared the different intestinal bacteria in LB medium, and centrifuged at 5000 × rpm at RT for 5 min when the bacteria at logarithmic growth period. After washed with PBS for two times, bacteria suspension was equally divided into three tubes with volume of 0.2 mL. Subsequently, the bacteria suspension was incubated with DDAV (10 μmol/L), β-lapachone (20 μmol/L) and DDAV (10 μmol/L), equal amount of organic solvent at 37 °C for 1 h. The content of organic solvent in the system shall not exceed 1%. Lastly, centrifuged at RT and washed the bacteria with PBS for three times, bacteria suspension was dropped on the slide glasses for fluorescence imaging with excitation at 633 nm and the collected windows were set as 645−690 nm.

2.7. The screening of Vanin-1 inhibitors

Ethanol extractions of 92 herbal medicines (10 μg/mL) were added into the reaction solution (consisting of 15 ng/mL Vanin-1 and 10 μmol/L DDAV in potassium phosphate buffer), respectively. After a co-incubation of 30 min, the fluorescence intensity of each plate was determined by BioTek Synergy H1 microplate reader ($\lambda_{ex}/\lambda_{em}$ = 600/670 nm).

The chemical components fraction of Cortex Fraxini was separated by Waters preparative HPLC with C18 column combined with an efficient HPLC method (mobile phase A: consisted of 10% methanol + 90% trifluoroacetic acid water; B: 100% methanol) at a flow rate of 10 mL/min. The following gradient condition was used: 0−5 min 85% A; 5−10 min 85%−80% A; 10−15 min 80%−65%A; 15−25 min 65% A; 25−30 min 65%−40% A; 30−35 min 40%−45% A; 35−40 min 40%−10% A, and the prepared fractions were further evaluated for the inhibitory effect on Vanin-1 using the procedure mentioned above,

respectively. Then, the key compound in Fr. 8 was isolated by HPLC and identified by NMR analysis. Finally, the IC_{50} value of oleuropein as a Vanin-1 inhibitor was evaluated based on the inhibitory effect in different concentrations.

3. Results

3.1. *The hydrolysis of DDAV by Vanin-1*

Firstly, the spectroscopic properties of DDAV toward Vanin-1 were investigated. As shown in Fig. 1B, DDAV exhibited a strong absorption peak at 480 nm, while the maximum absorption peak red-shifted to 620 nm after incubating with Vanin-1, accompanied by a prominent enhancement of the fluorescence intensity at 670 nm (Fig. 1C). Clearly, the distinct spectral response was ascribed to the specific cleavage of the recognition site of DDAV and release of the fluorophore DDAN (Φ = 0.135), the metabolism progress was further verified by HPLC analysis with help of standard of DDAN and HRMS analysis for the metabolite peak at m/z = 305.0261 $[M-H]^-$ (Supporting Information Fig. S1).

3.2. *The fluorescence behavior of DDAV toward Vanin-1*

Additionally, DDAV used as a molecular tool for evaluating Vanin-1 activity has been investigated in consideration of its sensitivity, selectivity and reliability. Firstly, the effect of pH and temperature on the hydrolysis reaction of DDAV in Vanin-1 were evaluated. As shown in Supporting Information Fig. S2A, the hydrolysis reaction mediated by Vanin-1 maintained stabilized efficiency at pH 5−8. Additionally, compared to the common physiological temperature (37 °C) a modestly elevated temperature (45 °C) facilitated the enzymatic reaction at a certain extent (Supporting Information Fig. S2B). All the above results indicated that the assays of Vanin-1 by DDAV was suitable under the physiological conditions (pH 7.4, 37 °C). Furthermore, as shown in Fig. 2A and B, the variation of fluorescence intensity at 670 nm displayed an excellent linearity with the increasing of Vanin-1 concentration from 0 to 50 ng/mL (R^2 = 0.9914) and a linear variation with the reaction times up to 110 min (Supporting Information Fig. S3), in favor of accurately monitoring Vanin-1 activity under various physiological conditions. Next, the specificity of DDAV was systemically evaluated among different hydrolase enzymes. As shown in Fig. 2C, only Vanin-1 could trigger a marked fluorescence enhancement at 670 nm, while other enzymes including Ls, HSA, BSA, CE1b, CE1c, CE2, CYP3A4, LAP, DPP4, Cas, β-Glc, β-Gla, GLU and PK displayed a negative response. Subsequently, chemical inhibition was investigated to further validate the selectivity of DDAV toward Vanin-1. As Supporting Information Fig. S4 illustrated, β-lapachone, as a specific inhibitor of Vanin-1, exhibited a strikingly inhibition toward the enzyme-activated hydrolysis reaction, while other inhibitors such as BNPP (general inhibitor for CEs), LPA (a specific inhibitor for CE2) and ketoconazole (a specific CYP3As inhibitor) could not exert effective inhibitory effects on the hydrolysis progress of DDAV. In addition, DDAV could exhibit a good stability among various biologically important ions or biomolecules (Fig. 2D), all of which could fully confirm that DDAV was an excellent specific probe for Vanin-1.

Meantime, the enzyme kinetic behavior of hydrolysis reaction of DDAV in Vanin-1 was well characterized. As depicted in Supporting Information Fig. S5, a classic Michaelis−Menten kinetics was observed for the metabolism of DDAV, with the K_m = 4.667 μmol/L, and V_{max} = 2.879 μmol/min/mg. Subsequently, the activity of Vanin-1 in different human organs was evaluated using DDAV among HLS9, HLuS9, HIS9, HKS9 and HBS9, respectively. As a result, intestine and kidney exhibited relatively high Vanin-1 activity (Supporting Information Fig. S6), which was well consistent with the previous report[8−10].

3.3. *Detecting urinary Vanin-1 level in kidney injury mice model using DDAV*

Recently, numerous studies have confirmed that urinary Vanin-1 could serve as an earlier and high-sensitive biomarker for kidney injury[36,37]. Although few optical imaging probes have been developed to investigate drug-induced acute kidney injury by *in situ* sensing superoxide anion, *N*-acetyl-β-D-glucosaminidase (NAG) and γ-glutamyl transferasein (GGT), convenient and rapid noninvasive detection of urinary biomarker (such as Vanin-1) *in vitro* based on sensitively fluorescence imaging techniques are

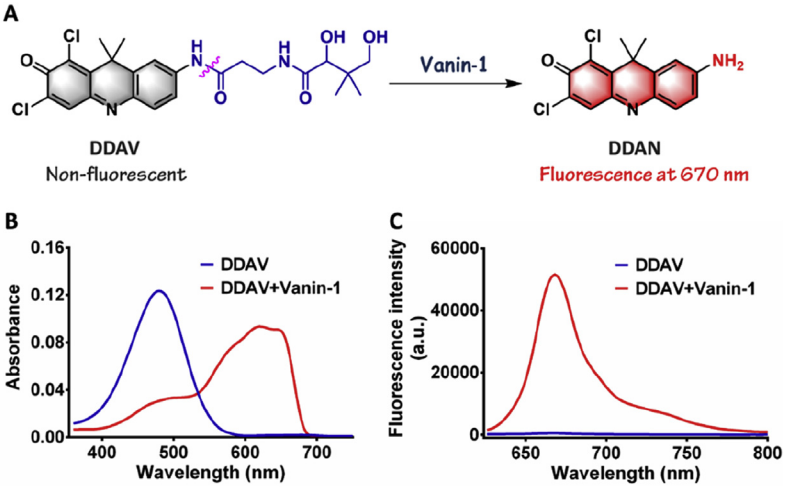

Figure 1 (A) Illustration of DDAV mediated by Vanin-1. The absorption (B) and fluorescence (C) spectra response of DDAV toward Vanin-1.

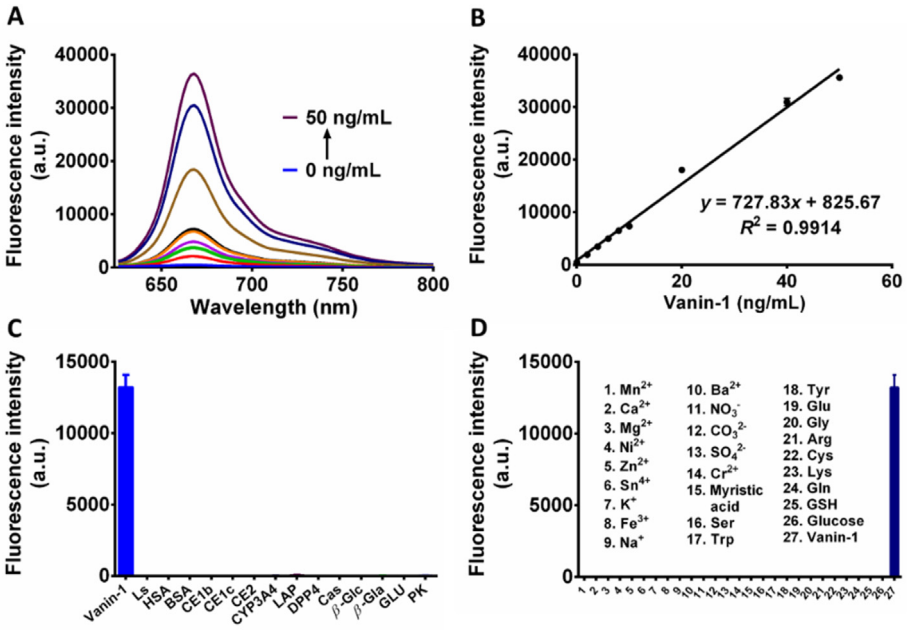

Figure 2 (A, B) Fluorescence response of DDAV toward different concentrations of Vanin-1 over a range from 0 to 50 ng/mL. (C) The selectivity assay of DDAV toward Vanin-1 among various hydrolysis enzymes. (D) The influence of various ions and biomolecules toward DDAV.

still lacking[38–41]. Herein, in order to further evaluate the diagnosis value of Vanin-1 for renal injury, an acute kidney injury animal model was established in C57BL/6 mice by administration of cisplatin primarily. As shown in Fig. 3A and B, the cisplatin-treated group displayed a significantly elevation for both blood urea nitrogen (BUN) and serum creatinine (sCr) levels than control group. In addition, Hematoxylin and Eosin (H&E) staining demonstrated a serious proximal tubule damage in cisplatin-treated group (Fig. 3C and D). Moreover, the conspicuous albumin expression was detected in urine by Western blots (Fig. 3E). All these results indicated that the cisplatin-induced kidney injury model was well established.

Simultaneously, urinary Vanin-1 was detected by DDAV. As shown in Fig. 3F, a sharply enhancement of Vanin-1 activity in urine for cisplatin group was observed, which were further confirmed by Western blots analysis (Supporting Information Fig. S7), and these results were well in accordance with both BUN and sCr detection for renal injury. Moreover, as shown in Fig. 3G, urinary Vanin-1 level exhibited a significantly and continuously increase after treatment with cisplatin within 72 h. Notably, the Vanin-1 level in urine of the control group was almost undetectable, exhibiting a distinct lower background and consequently higher signal to noise ratio than BUN and sCr.

3.4. *Bioimaging of Vanin-1 in living cells*

Next, the application potential of DDAV for imaging endogenous Vanin-1 in living cells was explored. Initially, DDAV exhibited very low cytotoxicity and superior biocompatibility to cultured cell lines by CCK8 assay (Supporting Information Fig. S8). Thereafter, the fluorescence imaging of endogenous Vanin-1 was conducted in MCT cells and LoVo cells. As shown in Fig. 4 and Supporting Information Fig. S9, both MCT and LoVo cells exhibited no fluorescence background, while a robust red fluorescence signal was detected in cells after the incubation with DDAV. Further, the fluorescence signal could be significantly suppressed by β-lapachone, which fully verified that the conspicuous fluorescence signal was originated from the specific metabolism of DDAV by Vanin-1.

3.5. *Visualization of Vanin-1 in vivo and screening of intestinal bacteria with high Vanin-1 expression*

Encouraged by the evident "light-up" NIR fluorescence signal and prominent performance in cellular fluorescence imaging, we further evaluated the *in vivo* imaging of DDAV in living mice. As depicted in Fig. 5A, after intraperitoneal administration of DDAV, a distinct fluorescence signal was clearly detected in the intestine region of mice. Next, after the clearance of DDAV *in vivo*, the inhibition experiments were performed in the same mouse by co-administration of β-lapachone and DDAV, as shown in Fig. 5A, the fluorescence intensity of inhibition group exhibited a significant decrease compared with the mouse without treatment of β-lapachone. These results fully indicated that the fluorescence signal in intestine was mediated by the endogenous Vanin-1 in mouse, and further confirmed the capability of DDAV in imaging Vanin-1 *in vivo*.

Additionally, the activity of Vanin-1 in feces was also determined using DDAV. As shown in Fig. 5B, all feces S9 samples originated from different mice could trigger an evidently fluorescence enhancement at 670 nm, indicating a high level of Vanin-1 in feces. Interestingly, after administration of antibiotic, the activity of Vanin-1 exhibited a significant reduce, along with the conspicuous decrease of intestinal bacteria (Fig. 5C and D), which results suggested that the Vanin-1 level in feces predominantly depended on intestinal bacteria and further implied that intestinal bacteria possessed high Vanin-1 expression.

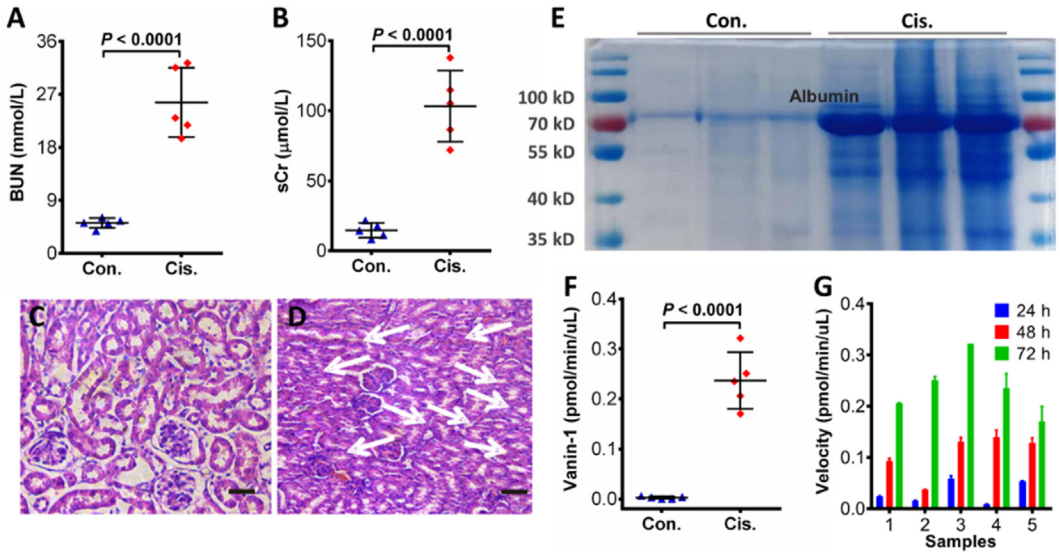

Figure 3 The level of (A) BUN and (B) sCr in the urine of control and cisplatin-treated C57BL/6 mice. (C, D) The H&E staining of kidney tissues for control group and cisplatin treated group, respectively. The scale bar is 100 μm. (E) The Western blot assay for the albumin in urine for control group and cisplatin treated group, respectively. (F) The activity of Vanin-1 in the urine of control and cisplatin-treated C57BL/6 mice. (G) The activity of Vanin-1 in urine during the C57 BL/6 mice treated with cisplatin in different time (24, 48, and 72 h).

Considering that intestinal bacteria had an abundant expression of Vanin-1 which was potentially related to the nonsteroidal anti-inflammatory drugs (NSAIDs) induced intestinal injury[14], the discovery of key bacteria in the intestine was invaluable in the forecast and prevention of relevant intestinal injury. Thereafter, using DDAV, we screened various common intestinal bacteria (Supporting Information Table S1). After incubating with DDAV, only bacteria 34A (*Enterococcus faecalis* 20247) displayed a

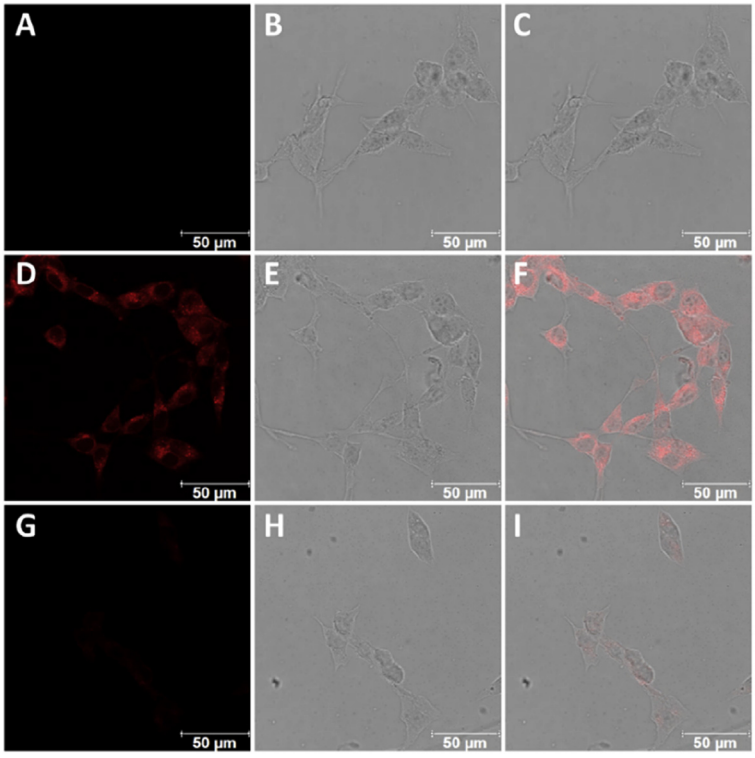

Figure 4 Fluorescence imaging of Vanin-1 in MCT cells. (A−C) MCT cells only. (D−F) MCT cells incubated with DDAV. (G−I) MCT cells pre-treated with β-lapachone before incubated with DDAV. The scale bar is 50 μm.

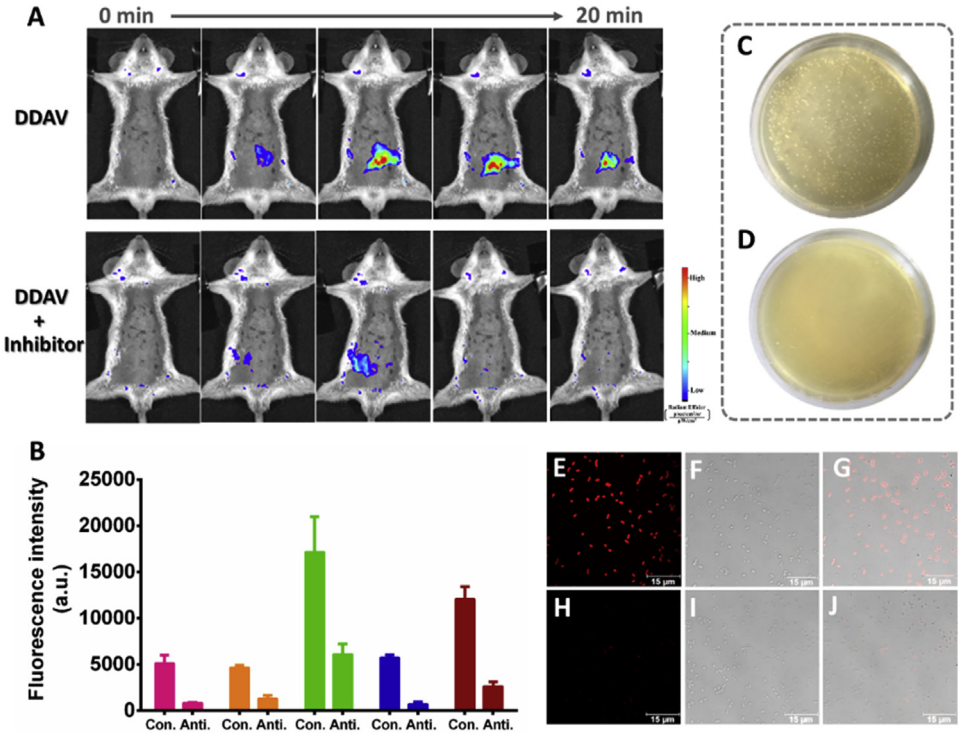

Figure 5 (A) The *in vivo* imaging of Vanin-1 in living mice, normal group: mouse was intraperitoneal injected of DDAV, inhibition group: mouse was treated with β-lapachone and DDAV. (B) The activity of Vanin-1 in feces S9 in the mice before and after treated with mixed antibiotic. (C, D) The plate cultivation for the intestinal bacteria before (C) and after (D) treated with mixed antibiotic. (E—G) The fluorescence imaging of Vanin-1 in *E. faecalis* 20247 after incubated with DDAV. (H—J) The fluorescence imaging of *E. faecalis* 20247 after pre-treated with β-lapachone.

remarkable fluorescence signal at 645—690 nm channel (Fig. 5E–G), and the fluorescence signal could be evidently suppressed by pretreated with Vanin-1 selective inhibitor β-lapachone, all the above results indicated that *E. faecalis* 20247 had an extensive expression of Vanin-1.

3.6. High-throughput screening of Vanin-1 inhibitors from herbal medicines based on DDAV

Importantly, Vanin-1 also serves as a key regulator in the progression of intestinal inflammatory reactions by producing cysteamine, the inhibition of Vanin-1 activity provides an attractive therapeutic intervention for the treatment of inflammatory bowel disease. Herein, a high-throughput screening method for Vanin-1 inhibitors was established, and 92 species of common medicinal herbs were subsequently determined for the inhibitory effect on Vanin-1. As shown in Fig. 6B and Supporting Information Table S2, well G4 (Cortex Fraxini) exhibited a significant inhibition on Vanin-1 (residual activity: 3.35%) among various herbal medicines. Inspired by the attractive primary screening results, we further identified the chemical constituents of Cortex Fraxini which was responsible for the Vanin-1 inhibitory. As shown in Fig. 6A and C, 10 fractions of Cortex Fraxini were obtained, and fraction 8 (Fr. 8) exhibited obvious inhibitory effect on Vanin-1 activity. Then, the target compound (CF—F8) within Fr. 8 was further purified and identified as oleuropein by NMR analysis (Supporting Information Figs. S15 and S16)[42]. Furthermore, the inhibition curve of oleuropein against Vanin-1 was performed and the IC_{50} value was calculated to 0.29 μmol/L (Fig. 6E). Altogether, DDAV also possessed a promising application in the rapidly screening of Vanin-1 inhibitors.

4. Discussion

In recent years, functional studies have revealed that Vanin-1 plays a critical role in various physiological and pathological processes. On the one hand, Vanin-1 is regarded as a disease biomarker for its remarkable up-regulation in the early phase of renal injury. On the other hand, Vanin-1 proved to be a pro-inflammatory factor in acute/chronic intestinal diseases due to its significant capacity in regulating oxidative stress and inflammation. Therefore, developing practical tools for real-time and accurate detecting endogenous Vanin-1 activity in various biosystems is invaluable and urgent, which would strongly facilitate further exploring Vanin-1's pathophysiology function even the diagnosis and therapies of Vanin-1-related diseases.

In this study, we designed and developed an off-on NIR fluorescent probe DDAV by conjugating pantothenic acid as a recognition moiety with DDAN. As expected, after hydrolysis of enzyme-triggered amide moiety mediated by Vanin-1, the bare amino group of the fluorophore as a strong electron donor was liberated, triggering a distinct fluorescence signal for the enhanced intramolecular charge transfer (ICT) effect (Fig. 1A). After the systematical evaluation, DDAV was proved to possess ultra-

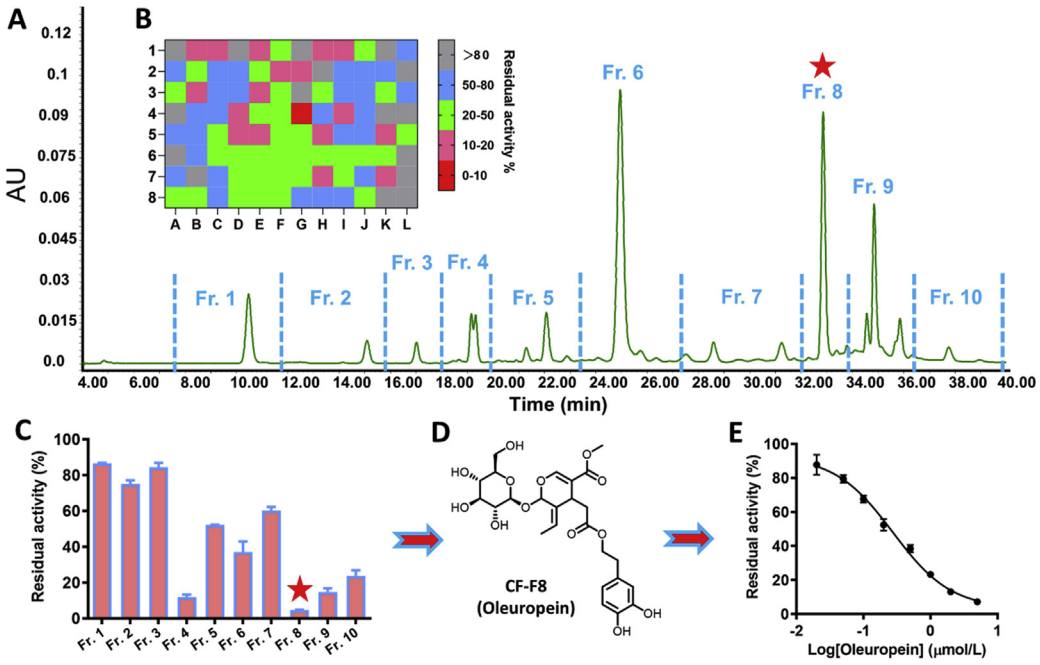

Figure 6 (A) HPLC chromatogram and 10 fractions of Cortex Fraxini. (B) Inhibitory effect evaluation of 92 medicinal herbs towards Vanin-1. (C) Inhibitory effect evaluation of 10 fractions of Cortex Fraxini towards Vanin-1. (D) Chemical structure of oleuropein. (E) Inhibition curve of oleuropein (IC_{50}) toward Vanin-1.

specificity to Vanin-1 among various common enzymes in the human body and the formation of DDAN mediated by Vanin-1 was highly time- and enzyme-dependent, which in favor of precise quantification of Vanin-1 activity in complex biosamples. Additionally, the metabolism of DDAV by Vanin-1 followed classical Michaelis−Menten kinetics evidencing by the Eadie–Hofstee plots, the ideal kinetic behaviors and good catalytic velocity further ensure its practicability in quantitative detecting Vanin-1 without substrate inhibition. At last, the applications of DDAV for bioimaging Vanin-1 in living cells and mice were evaluated, the results indicated that DDAV could serve as an efficient molecular tool for *in situ* visualizing endogenic Vanin-1 *in vitro* and *in vivo*. All above results fully demonstrated that DDAV could serve as practical probe for excellent specific and accurate monitoring Vanin-1 activity in complex biological systems.

Recent studies have verified that urinary Vanin-1, derived from damaged tubular kidney cells, can consequently serve as an earlier and sensitive biomarker for kidney injury. We subsequently evaluated the application of DDAV for renal injury diagnosis. Herein, a cisplatin-induced kidney injury model was successfully established, then the urinary Vanin-1 was evaluated using DDAV, it was found that the cisplatin-induced mice urinary Vanin-1 level displayed a remarkable increase than control group, which were further verified by Western blot and highly consistent with traditional detection methods (BUN and sCr) for kidney injury. Significantly, the kidney injury could be detected by DDAV at 24 h (Fig. 3G) which showed more sensitive than BUN and sCr testing method. Further, the Vanin-1 level in urine of the control group was close to zero, implying that slight increase of urinary Vanin-1 could directly indicate the impairment of kidney, which was pivotal for diagnosis renal injury at a very early stage. Above all, these results verified that DDAV could serve as a practical tool for the earlier diagnosis of kidney injury with a high degree of sensitivity.

Notably, due to the strongly inhibition of γ-GCS (γ-glutamylcysteine synthetase) by the metabolite (cysteamine) of Vanin-1, intestinal Vanin-1 was regarded as a major pro-inflammatory mediator in varied intestine inflammation, including the common NSAIDs-induced intestinal injury. In this work, we investigated Vanin-1 level in feces samples, it was found that the Vanin-1 vitality in feces predominantly depended on intestinal bacteria. Next, *E. faecalis* 20247 was screened out which had an extensive expression of Vanin-1 from 27 species common intestinal bacteria using DDAV, the results indicated that *E. faecalis* 20247 as a vital bacterium, should be serious tested before administration of NSAIDs in clinic.

As mentioned above, Vanin-1 serve as a vital regulator of intestinal inflammation, and the manipulation of Vanin-1 activity with the aid of selective inhibitor may prove to be a new therapeutic strategy for inflammatory bowel disease. We subsequently established a high-throughput screening assay for Vanin-1 inhibitors discovery based on DDAV. Then, 92 species of common medicinal herbs were selected for assessment and Cortex Fraxini was eventually found that exhibited a strongly inhibitory effect on Vanin-1. Further, after a series of separation and analysis experiments, the key chemical component which responsible for the Vanin-1 inhibitory in Cortex Fraxini was isolated and identified as oleuropein, which exhibited remarkable inhibitory effect (IC_{50} value: 0.29 μmol/L) on Vanin-1 and held great promise as novel agent for the potential application in intestinal inflammation therapy. In one word, all our findings provided useful information for the physiological function of Vanin-1 in human and its relationship with various diseases.

5. Conclusions

In summary, an enzyme-activated NIR fluorescent probe DDAV has been developed for ultra-sensitive and high specific sensing Vanin-1 activity in various complex biosystems. DDAV could be applied to the early diagnosis of kidney injury by assaying the urinary Vanin-1 activity. Additionally, DDAV could realize the real-time imaging of Vanin-1 *in vitro* and *in vivo*. Furthermore, *E. faecalis* 20247, a general intestinal bacterium, with high expression of Vanin-1 was successfully screened out based on the DDAV imaging. Finally, oleuropein as a novel potent inhibitor was discovered from natural herbal medicines by high-throughput screening method using DDAV. In one word, DDAV was proved to be a novel promising tool for detecting Vanin-1 levels *in vitro* and *in vivo*, which could be further used for the early diagnosis of kidney injury, discovery of functional microorganisms, as well as the development of novel Vanin-1 inhibitors for therapy of inflammatory bowel disease in clinic.

Acknowledgments

This work was financially supported by National Natural Science Foundation of China (Nos. 81930112 and 82004211), State Key Laboratory of Fine Chemicals KF1912, Distinguished professor of Liaoning Province, Dalian Science and Technology Leading Talents Project (2019RD15, China) and the Open Research Fund of the School of Chemistry and Chemical Engineering, Henan Normal University (2021YB07).

Author contributions

Xiaochi Ma, Tian Xie and Lei Feng conceived and supervised the project. Zhenhao Tian, Fei Yan and Xiangge Tian contributed to the experimental designs, performed experiments, analyzed data, interpreted the results and wrote the original manuscript; Tian Xie, Jingnan Cui, Sa Deng, Baojing Zhang and Shanshan Huang critically revised the manuscript. All authors contributed and reviewed the results and approved the final manuscript.

Conflicts of interest

The authors have no conflicts of interest to declare.

Appendix A. Supporting information

Supporting information to this article can be found online at https://doi.org/10.1016/j.apsb.2021.06.004.

References

1. AurrandLions M, Galland F, Bazin H, Zakharyev VM, Imhof BA, Naquet P. Vanin-1, a novel GPI-linked perivascular molecule involved in thymus homing. *Immunity* 1996;**5**:391−405.
2. Pitari G, Malergue F, Martin F, Philippe JM, Massucci MT, Chabret C, et al. Pantetheinase activity of membrane-bound Vanin-1: lack of free cysteamine in tissues of Vanin-1 deficient mice. *FEBS Lett* 2000;**483**:149−54.
3. Berruyer C, Pouyet L, Millet V, Martin FM, LeGoffic A, Canonici A, et al. Vanin-1 licenses inflammatory mediator production by gut epithelial cells and controls colitis by antagonizing peroxisome proliferator-activated receptor gamma activity. *J Exp Med* 2006;**203**:2817−27.
4. van Diepen JA, Jansen PA, Ballak DB, Hijmans A, Hooiveld GJ, Rommelaere S, et al. PPAR-alpha dependent regulation of vanin-1 mediates hepatic lipid metabolism. *J Hepatol* 2014;**61**:366−72.
5. Rommelaere S, Millet V, Gensollen T, Bourges C, Eeckhoute J, Hennuyer N, et al. PPARalpha regulates the production of serum Vanin-1 by liver. *FEBS Lett* 2013;**587**:3742−8.
6. Nitto T, Onodera K. The linkage between coenzyme A metabolism and inflammation: roles of pantetheinase. *J Pharmacol Sci* 2013;**123**:1−8.
7. Chen SY, Zhang WX, Tang CQ, Tang XL, Liu L, Liu C. Vanin-1 is a key activator for hepatic gluconeogenesis. *Diabetes* 2014;**63**:2073−85.
8. Bartucci R, Salvati A, Olinga P, Boersma YL. Vanin 1: its physiological function and role in diseases. *Int J Mol Sci* 2019;**20**:3891.
9. Roisin-Bouffay C, Castellano R, Valero R, Chasson L, Galland F, Naquet P. Mouse vanin-1 is cytoprotective for islet beta cells and regulates the development of type 1 diabetes. *Diabetologia* 2008;**51**:1192−201.
10. Rommelaere S, Millet V, Rihet P, Atwell S, Helfer E, Chasson L, et al. Serum pantetheinase/Vanin levels regulate erythrocyte homeostasis and severity of malaria. *Am J Pathol* 2015;**185**:3039−52.
11. Hosohata K, Ando H, Fujimura A. Urinary Vanin-1 as a novel biomarker for early detection of drug-induced acute kidney injury. *J Pharmacol Exp Therapeut* 2012;**341**:656−62.
12. Hosohata K, Ando H, Fujimura A. Early detection of renal injury using urinary vanin-1 in rats with experimental colitis. *J Appl Toxicol* 2014;**34**:184−90.
13. Washino S, Hosohata K, Oshima M, Okochi T, Konishi T, Nakamura Y, et al. A novel biomarker for acute kidney injury, Vanin-1, for obstructive nephropathy: a prospective cohort pilot study. *Int J Mol Sci* 2019;**20**:899.
14. Martin F, Penet MF, Malergue F, Lepidi H, Dessein A, Galland F, et al. Vanin-1$^{-/-}$ mice show decreased NSAID- and Schistosoma-induced intestinal inflammation associated with higher glutathione stores. *J Clin Invest* 2004;**113**:591−7.
15. Wittwer C, Wyse B, Hansen RG. Assay of the enzymatic-hydrolysis of pantetheine. *Anal Biochem* 1982;**122**:213−22.
16. Dupre S, Chiaraluce R, Nardini M, Cannella C, Ricci G, Cavallini D. Continuous spectrophotometric assay of pantetheinase activity. *Anal Biochem* 1984;**142**:175−81.
17. Liu HW, Chen LL, Xu CY, Li Z, Zhang HY, Zhang XB, et al. Recent progresses in small-molecule enzymatic fluorescent probes for cancer imaging. *Chem Soc Rev* 2018;**47**:7140−80.
18. Zhao JH, Chen JW, Ma SN, Liu QQ, Huang LX, Chen XN, et al. Recent developments in multimodality fluorescence imaging probes. *Acta Pharm Sin B* 2018;**8**:320−38.
19. Tian ZH, Yan QS, Feng L, Deng S, Wang C, Cui JN, et al. A far-red fluorescent probe for sensing laccase in fungi and its application in developing an effective biocatalyst for the biosynthesis of antituberculous dicoumarin. *Chem Commun* 2019;**55**:3951−4.
20. Wu XF, Shi W, Li XH, Ma HM. Recognition moieties of small molecular fluorescent probes for bioimaging of enzymes. *Accounts Chem Res* 2019;**52**:1892−904.
21. Feng L, Ning J, Tian XG, Wang C, Zhang LY, Ma XC, et al. Fluorescent probes for bioactive detection and imaging of phase II metabolic enzymes. *Coord Chem Rev* 2019;**399**:213026.
22. Jiang A, Chen G, Xu J, Liu YX, Zhao GH, Liu ZJ, et al. Ratiometric two-photon fluorescent probe for in situ imaging of carboxylesterase (CE)-mediated mitochondrial acidification during medication. *Chem Commun* 2019;**55**:11358−61.
23. Ning J, Wang W, Ge GB, Chu P, Long FD, Yang YL, et al. Target enzyme-activated two-photon fluorescent probes: a case study of CYP3A4 using a two-dimensional design strategy. *Angew Chem Int Ed* 2019;**58**:9959−63.
24. Tian ZH, Ding LL, Li K, Song YQ, Dou TY, Hou J, et al. Rational design of a long-wavelength fluorescent probe for highly selective

sensing of carboxylesterase 1 in living systems. *Anal Chem* 2019;**91**: 5638−45.
25. Chen SQ, Dong GQ, Wu SC, Liu N, Zhang WN, Sheng CQ. Novel fluorescent probes of 10-hydroxyevodiamine: autophagy and apoptosis-inducing anticancer mechanisms. *Acta Pharm Sin B* 2019;**9**: 144−56.
26. Lin YX, Gao YQ, Ma Z, Li ZZ, Tang CC, Qin XJ, et al. Bioluminescent probe for detection of starvation-induced pantetheinase upregulation. *Anal Chem* 2018;**90**:9545−50.
27. Qian J, Teng ZD, Wang JM, Zhang L, Cao T, Zheng L, et al. Visible to near-infrared emission ratiometric fluorescent probe for the detection of Vanin-1 *in vivo*. *ACS Sens* 2020;**5**:2806−13.
28. Qian J, Zhang L, Wang JM, Teng ZD, Cao T, Zheng L, et al. Red emission ratio fluorescent probe for the activity of vanin-1 and imaging *in vivo*. *J Hazard Mater* 2021;**401**:123863.
29. Yang YT, Hu YM, Shi W, Ma HM. A near-infrared fluorescence probe for imaging of pantetheinase in cells and mice *in vivo*. *Chem Sci* 2020; **11**:12802−6.
30. Ning J, Liu T, Dong PP, Wang W, Ge GB, Wang B, et al. Molecular design strategy to construct the near-infrared fluorescent probe for selectively sensing human cytochrome P450 2J2. *J Am Chem Soc* 2019;**141**:1126−34.
31. Tong HJ, Lou KY, Wang W. Near-infrared fluorescent probes for imaging of amyloid plaques in Alzheimer's disease. *Acta Pharm Sin B* 2015;**5**:25−33.
32. Li HD, Yao QC, Sun W, Shao K, Lu Y, Chung J, et al. Aminopeptidase N activatable fluorescent probe for tracking metastatic cancer and image-guided surgery *via in situ* spraying. *J Am Chem Soc* 2020;**142**: 6381−9.
33. Tian ZH, Feng L, Li L, Tian XG, Cui JN, Zhang HL, et al. Visualized characterization of bacterial penicillin G acylase for the hydrolysis of beta-lactams using an activatable NIR fluorescent probe. *Sensor Actuator B Chem* 2020;**310**:127872.
34. Huang JG, Jiang YY, Li JC, He SS, Huang JS, Pu KY. A renal-clearable macromolecular reporter for near-infrared fluorescence imaging of bladder cancer. *Angew Chem Int Ed* 2020;**59**: 4415−20.
35. Feng L, Tian ZH, Zhang M, He X, Tian XG, Yu ZL, et al. Real-time identification of gut microbiota with aminopeptidase N using an activable NIR fluorescent probe. *Chin Chem Lett* 2021;**32**:3053−6.
36. Hosohata K, Ando H, Fujiwara Y, Fujimura A. Vanin-1; a potential biomarker for nephrotoxicant-induced renal injury. *Toxicology* 2011; **290**:82−8.
37. Hosohata K, Washino S, Kubo T, Natsui S, Fujisaki A, Kurokawa S, et al. Early prediction of cisplatin-induced nephrotoxicity by urinary vanin-1 in patients with urothelial carcinoma. *Toxicology* 2016;**359**: 71−5.
38. Huang JG, Li JC, Lyu Y, Miao QQ, Pu KY. Molecular optical imaging probes for early diagnosis of drug-induced acute kidney injury. *Nat Mater* 2019;**18**:1133−43.
39. Lv Y, Cheng D, Su DD, Chen M, Yin BC, Yuan L, et al. Visualization of oxidative injury in the mouse kidney using selective superoxide anion fluorescent probes. *Chem Sci* 2018;**9**:7606−13.
40. Huang JG, Lyu Y, Li JC, Cheng PH, Jiang YY, Pu KY. A renal-clearable duplex optical reporter for real-time imaging of contrast-induced acute kidney injury. *Angew Chem Int Ed* 2019;**58**: 17796−804.
41. Cheng PH, Chen W, Li SH, He SS, Miao QQ, Pu KY. Fluoro-photoacoustic polymeric renal reporter for real-time dual imaging of acute kidney injury. *Adv Mater* 2020;**32**:1908530.
42. Gariboldi P, Jommi G, Verotta L. Secoiridoids from *Olea europaea*. *Phytochemistry* 1986;**25**:865−9.